Supplementary Information

Empirical Cumulative Density Function

The main strategy used in this study to illustrate the magnitude clustering observed in event pair comparisons is via an empirical cumulative density function (ECDF) of the earthquake magnitudes (Xiong et al., 2023). The ECDF is a commonly used non-parametric statistical method for visualizing the distribution of a dataset. This distribution doesn't make any prior assumptions about the probability distribution of the data, but rather simply relies on the organization of the dataset from the smallest to the largest value in order to visualize distribution trends.

To examine the ECDF of our earthquake catalog data, we began by sorting the event magnitudes from smallest to largest and marking where the event falls within the cumulative distribution of magnitude. We then re-sorted the catalog by time in order to compare the cumulative magnitude positions of subsequent events in the time-ordered catalog. The resulting plot organizes each earthquake magnitude m_i along the x-axis, and compares it to the magnitude of the subsequent event m_{i+1} in a time-ordered catalog on the y-axis. Plotting this comparison for all event pairs in the large dataset (hundreds of thousands of events in each catalog), we can then visualize trends in how the subsequent event magnitude is similar to the one of the event that occurred just before it.

Because the amount of events in the dataset is so large, plotting all event comparisons as individual points makes it difficult to visualize the data trends due to the density of data points. For this reason, we created bins for each 20% range of magnitudes on each axis and calculated the number of event pair data points that fall into each magnitude range bin. Heatmaps are visualized by assigning red or blue to bins based on the catalog's real difference from the mean that would be expected for a bin if there were a uniform distribution of events across the magnitude range (total number of pairs

divided by the number of bins). For comparison, randomly shuffling the time order of events before comparing the magnitudes should result in no significant deviation from a uniform distribution.

This organization of magnitude range bins naturally creates a line diagonally across the middle of the plot where the range of the subsequent event magnitude is similar to that of the event before it, which is what we expect for magnitude clustering. The ECDF plots in the main text show that for both catalogs, there are significantly more event pairs that fall along this line of similar magnitudes than pairs that fall into bins where the magnitudes are significantly different from each other. Furthermore, the large number of event comparisons, along with a version of the plots where the events are randomized in time wherein these same trends are not observed, establishes a statistical significance to this trend. This plotting method is also useful for showing that similar magnitude correlations occur throughout the entire range of magnitudes in the catalog, not just for smaller events. In fact, the largest percent difference from the mean for similar magnitude range bins occurs in the largest 20% of event magnitudes.

Rate-Dependent Catalog Completeness

Quality determination of an earthquake catalog's magnitude of completeness (m_c), along with filtering for the effects of short-term aftershock incompleteness (STAI), is essential to this study, as incompleteness in the catalog could lead to spurious magnitude correlations. We have determined the m_c and filtered for STAI via multiple methods mentioned in the main text of this paper, including the maximum curvature (Wiemer, 2000) and b-value stability (Cao and Gao, 2002; Woessner, 2005) methods for determining an overall m_c value, and implementing interevent time-based filters to account for STAI. These methods of determining the m_c are based on analysis of the catalog's frequency-magnitude distribution (FMD).

A previous study by Hainzl (2016) has sought additional ways to account for STAI in earthquake catalogs by developing a rate-dependent m_c value that varies in time based upon the earthquake rate, resulting in an improved temporal resolution of the m_c compared to those that are based mainly on the FMD. To test whether this type of approach has any significant effect on the amount of magnitude clustering observed, we applied the Hainzl method to our studied earthquake catalogs and completed our ECDF analysis on the modified catalogs.

The Hainzl method defines a catalog as complete for magnitudes $m \geq m_{c0}$ where the minimum completeness magnitude m_{c0} is recorded with a probability p_c. The time-varying m_c value then is based on a maximum earthquake rate r_{max} related to the probability p_c by the equation:

$$r_{max} = \frac{-ln(p_c)}{\Delta t}$$

where any time period with a seismicity rate r_{max} will be incomplete. The theoretical basis for the completeness magnitude $m_c$is then defined by:

$$m_c(t) = m - \frac{1}{b} log(\frac{r_{max}}{K}) - \frac{p}{b} log(t + c)$$

where $K, b, c,$ and p are sequence-dependent constants. To apply this method to our catalogs, we explicitly followed all steps of the algorithm outlined in the "Algorithm to Estimate M_c Based on Catalog Data" section of the Hainzl (2016) paper using the associated MATLAB code provided by Hainzl.

Results of this method for the Southern California catalog are shown in Figures S2 and S3. Figure S2 displays how the m_c varies over the entire time frame of the catalog, and Figure S3 shows the results of the ECDF analysis after removing from the catalog events that do not exceed the m_c value associated with the time of the event. This method of filtering results in a similar amount of magnitude clustering observed in both catalogs.

ETAS Catalogs Artificially Adjusted to Introduce Incompleteness

Synthetic earthquake catalogs created using ETAS are useful for testing the effects of different forms of catalog incompleteness, with a variety of ways to force incompleteness into the catalog. For example, previous studies have accomplished this by varying the ETAS parameters that are most likely to be affected by incompleteness (Nandan, Ouillon and Sornette, 2019). Others have forced incompleteness by removing events for a blind time after an earthquake as determined by a relation to the event's magnitude (Hainzl, 2021; Lippiello, 2018). As another test of whether incompleteness in the ETAS catalogs can give rise to artificial magnitude correlations, we created an ETAS catalog based on the Southern California catalog with tapered incompleteness. The tapering occurred linearly over 1 magnitude unit, with 100% events being retained above the upper threshold, 0% of events being retained below the lower threshold, and a linearly decreasing percentage from the upper to the lower limit. This was implemented with several strategies to mimic overall catalog incompleteness as well as STAI, with the lower limit being set at a static value for the overall catalog incompleteness, and the upper limit being adjusted over time based on the equation outlined in Helmstetter (2006) for the STAI. We attempted these strategies with and without any of our other filtering methods for STAI. The results, shown in Figures S8 and S9, demonstrate that forcing catalog incompleteness based on either of these strategies does not give rise to artificial magnitude correlations.

Supplementary Figures

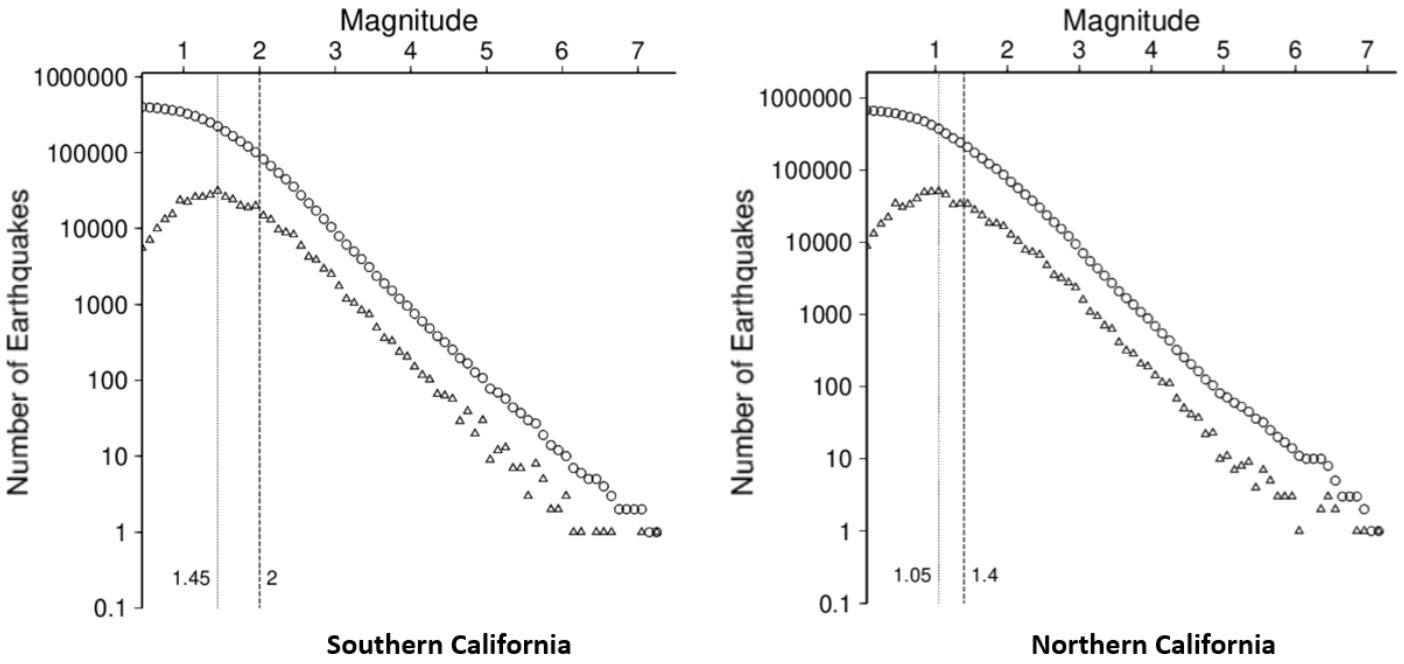

Figure S1: Frequency-magnitude distribution (FMD) of each catalog, used to determine the catalog-specific magnitude of completeness (m_c). The lighter vertical dotted line depicts the FMD using the maximum curvature method. The darker vertical dotted line depicts the FMD using the b-value stability method. The latter method was used for our analysis in order to provide a more conservative estimate of the m_c. Regardless of the FMD method chosen, the magnitude clustering signature remains prominent even after applying our filtering methods.

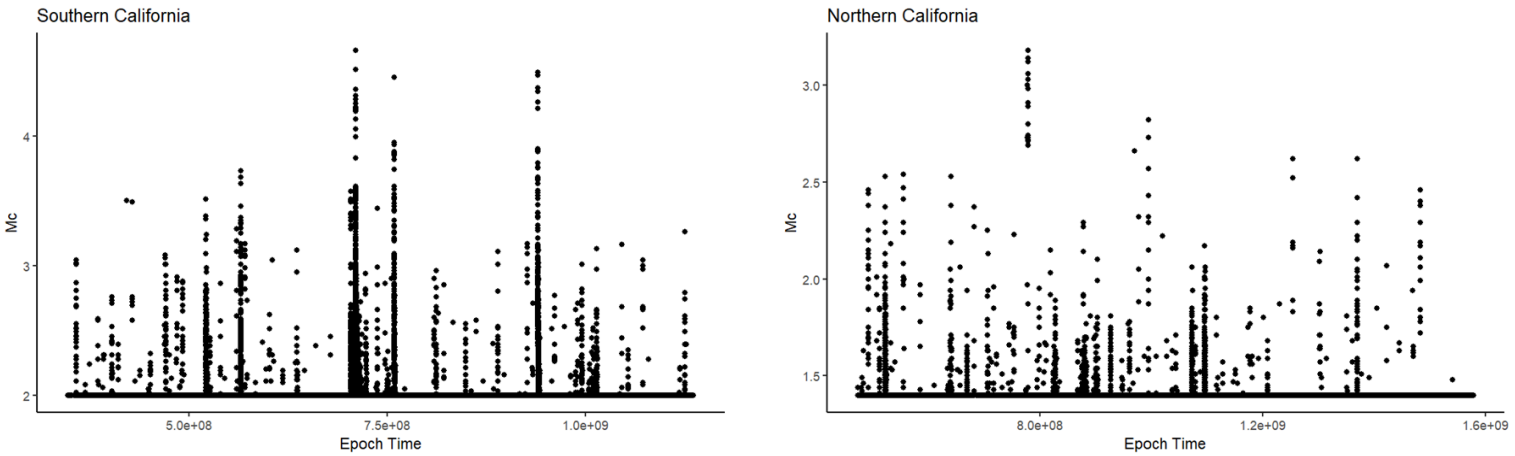

Figure S2: Rate-dependent magnitude of completeness (m_c) of the Southern California and Northern California catalogs. Processed according to Hainzl (2016).

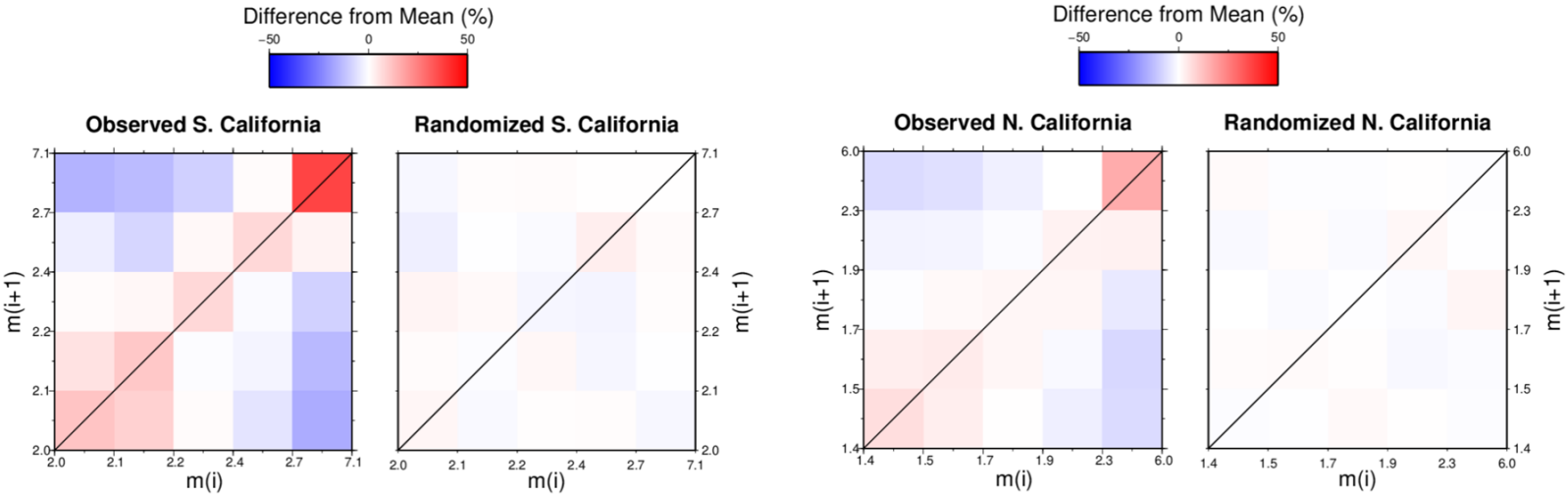

Figure S3: ECDF results for Southern and Northern California catalogs filtered using Hainzl (2016) method of rate-dependent magnitude of completeness method.

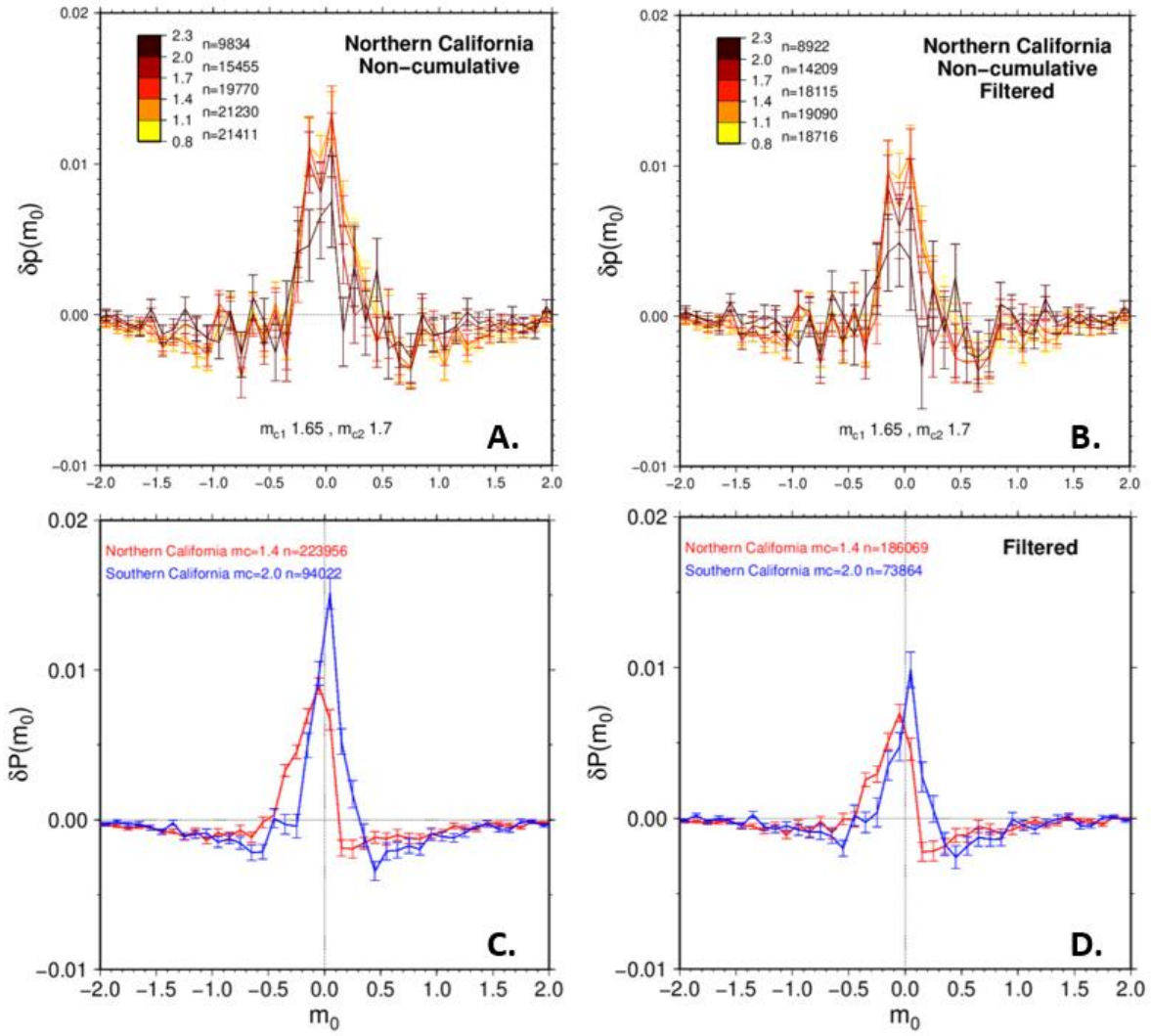

Figure S4: **A** Non-cumulative distribution of difference in probability between the observed catalog and a randomly shuffled version, $\delta p(m_0)$ as a function of magnitude difference (m_0) for the southern California catalog. The distribution is shown at various magnitude of completeness thresholds (corresponding to the different colored lines). $m_c =$ magnitude of completeness, n = number of events. Error bars correspond to the 1 standard deviation confidence interval. **B** Same as **A** but after applying filters to account for catalog incompleteness and short-term aftershock incompleteness (STAI). **C** Comparison of the cumulative distribution plots of both the Northern and Southern California study areas at the respective magnitudes of completeness of each catalog. **D** same as **C** but after applying filters for incompleteness/STAI.

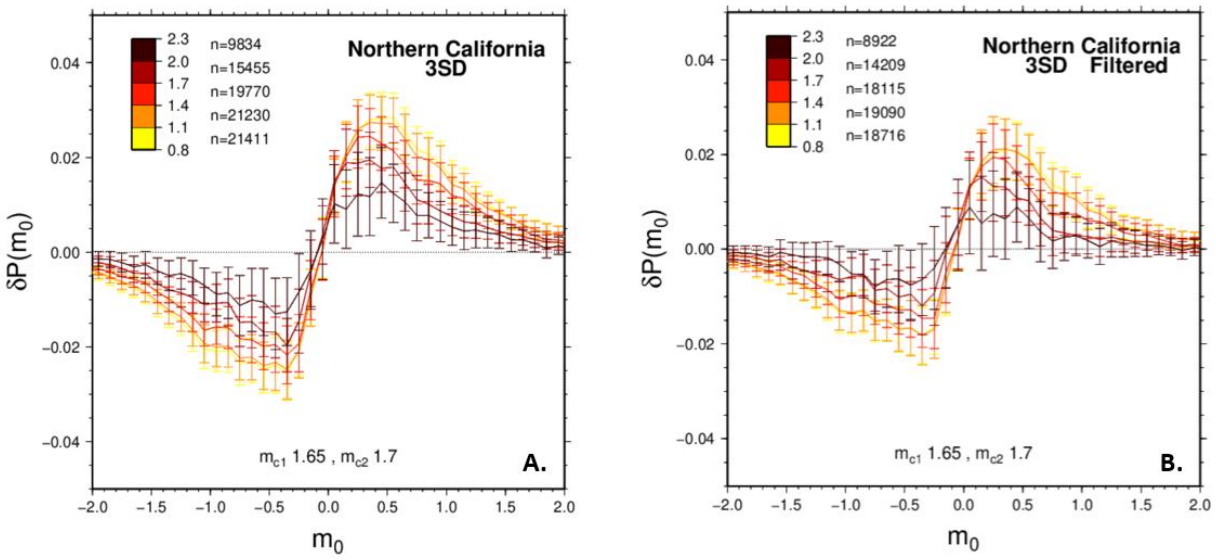

Figure S5: **A** Cumulative distribution of difference in probability between the observed catalog and a randomly shuffled version, $\delta p(m_0)$ as a function of magnitude difference (m_0) with a 3σ standard deviation for the Northern California catalog. $m_c =$ magnitude of completeness, n = number of events. Error bars correspond to the 1 standard deviation confidence interval. **B** Same as **A** but after applying filters to account for catalog incompleteness and short-term aftershock incompleteness (STAI).

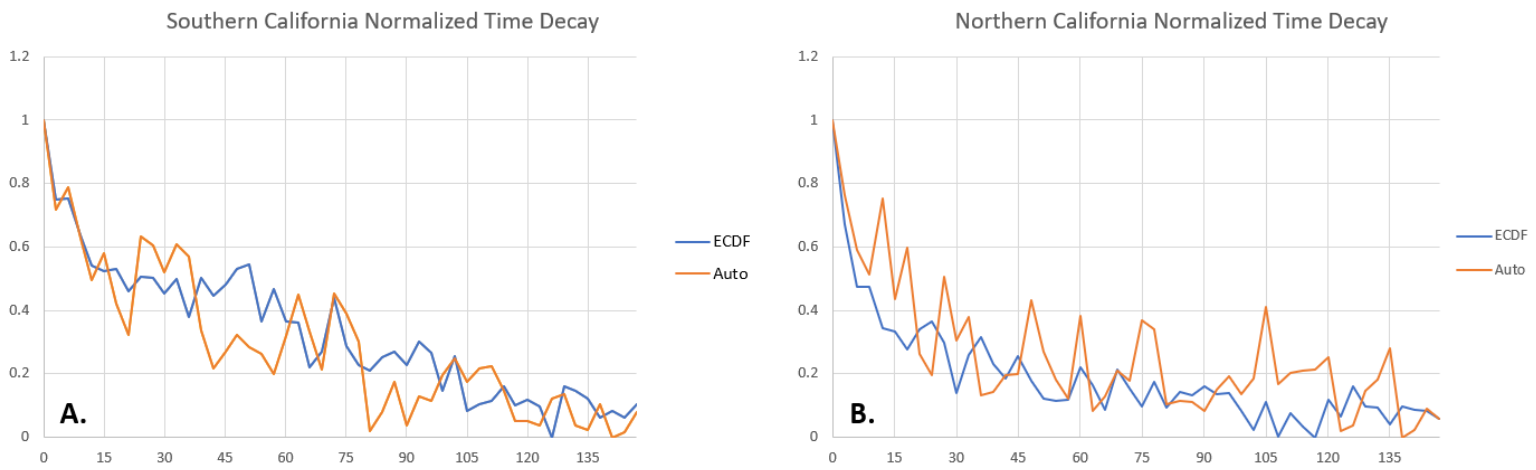

Figure S6: Rescaled time decay curves using min-max normalization for the ECDF (blue) and Autocorrelation (orange) methods in both the Southern California A and Northern California B catalogs.

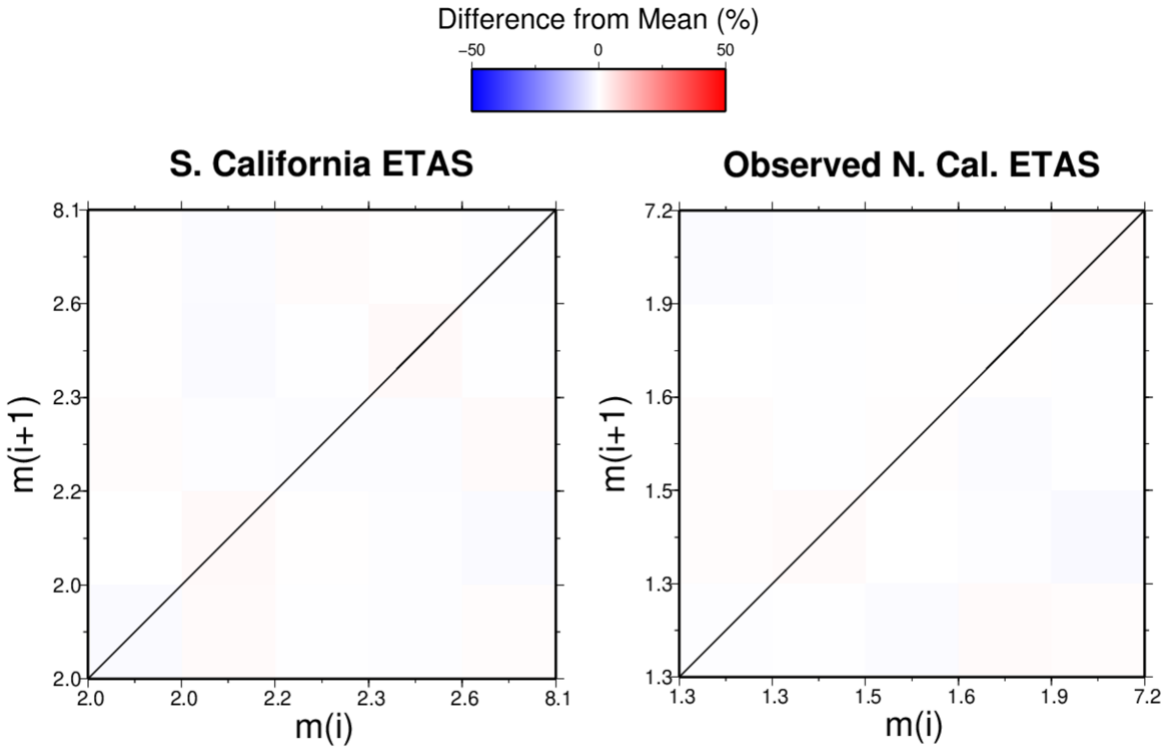

Figure S7: Empirical cumulative distribution function (ECDF) comparisons for synthetic ETAS catalogs fit to the Southern California catalog **A**, and the Northern California catalog **B.**

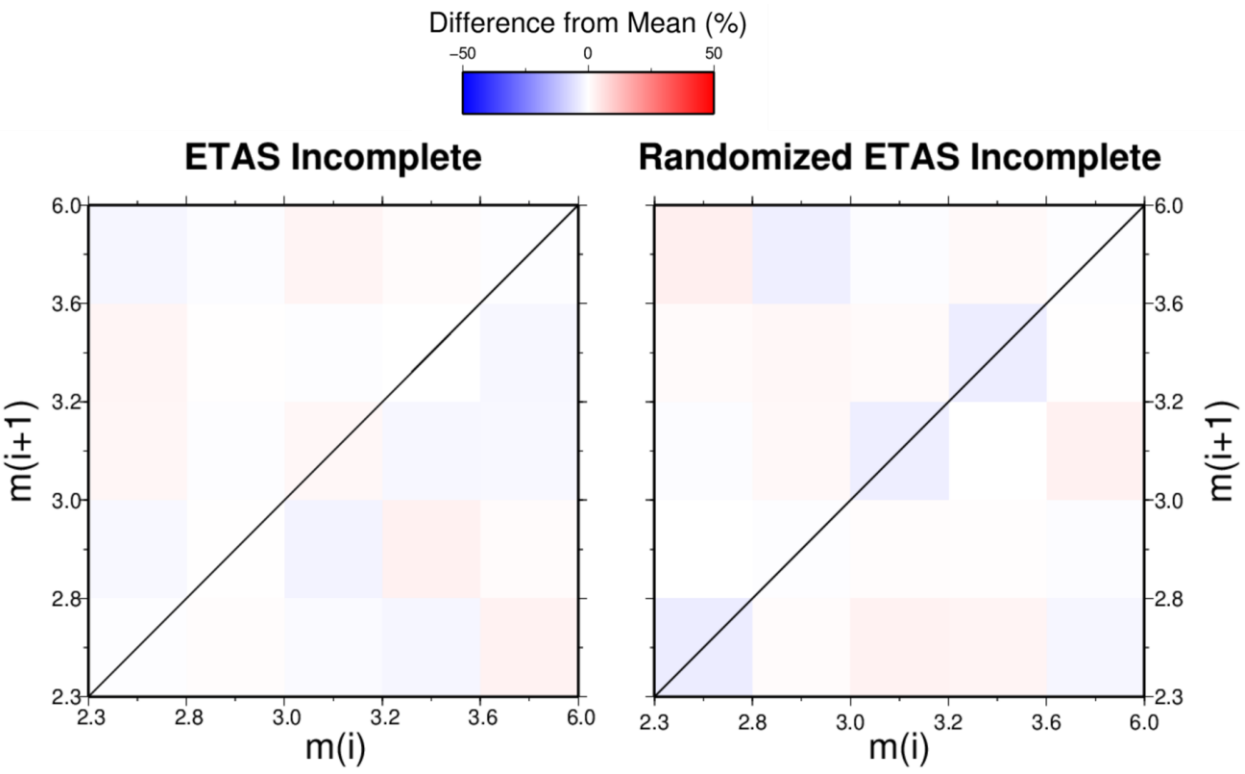

Figure S8: Empirical cumulative distribution function (ECDF) comparisons for synthetic ETAS catalogs fit to the Southern California catalog with incompleteness artificially added by progressively removing smaller events from the catalog.

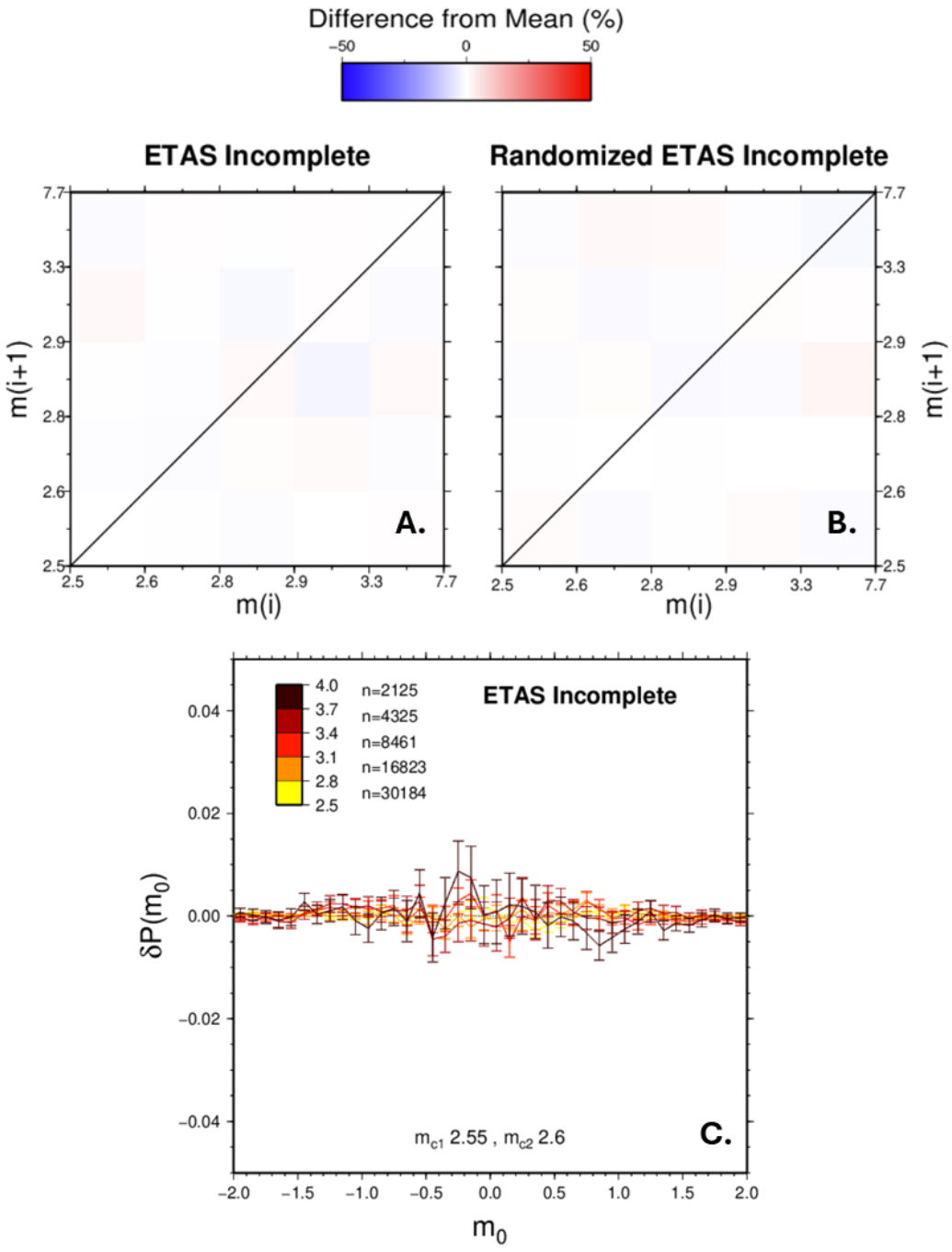

Figure S9: Empirical cumulative distribution function (ECDF) (**A.** and **B.**) and cumulative distribution function (**C.**) comparisons for synthetic ETAS catalogs fit to the Southern California catalog with incompleteness artificially added by tapering that removes events starting at the calculated Helmsetter incompleteness magnitude with 100% removed at 1 magnitude unit below it.

Supplementary Tables

Table S1: Regression Statistics of ECDF Decay Plots

	Northern California			Southern California		
	Linear	**Logarithmic**	**Power-law**	**Linear**	**Logarithmic**	**Power-law**
	Interevent Number Decay			**Interevent Number Decay**		
P-value	8.19×10^{-15}	5.73×10^{-16}	2.00×10^{-16}	1.16×10^{-8}	1.18×10^{-7}	3.52×10^{-11}
F-Statistic	83.84	93.87	148.2	38.84	32.66	55.66
R-squared	0.4611	0.4892	0.602	0.2838	0.25	0.3622
	Time Decay			**Time Decay**		
P-value	1.82×10^{-6}	1.11×10^{-16}	2.40×10^{-14}	2.44×10^{-13}	1.05×10^{-13}	8.57×10^{-11}
F-Statistic	29.51	90.65	48.9	55.56	60.33	29.52
R-squared	0.551	0.921	0.927	0.846	0.885	0.885
	Distance Decay			**Distance Decay**		
P-value	2.33×10^{-8}	8.02×10^{-8}	2.56×10^{-6}	9.95×10^{-10}	2.32×10^{-8}	1.49×10^{-6}
F-Statistic	82.88	46.29	23.80	122.61	54.45	25.76
R-squared	0.897	0.939	0.944	0.928	0.948	0.948

Table S2: ETAS Parameters

Parameter	Significance	Value
m_c	Magnitude of completeness	2.0 (S. Cal), 1.4 (N. Cal.)
$log_{10}(\mu)$	Background seismicity rate	-5.97
$log_{10}(k_0)$	Governs the expected number of aftershocks per event	-2.63
α	Effect of an earthquake's magnitude on its expected number of aftershocks	1.87
$log_{10}(c)$	Parameter governing aftershock rate	-2.52
ω	Spatial parameter of aftershocks	-0.02
$log_{10}(d)$	Spatial equivalent to c	-0.86
$log_{10}(\tau)$	Smoothness parameter	3.57
γ	Defines the spatial kernel	1.35
ρ	Describes the decay rate of aftershocks	0.67

References:

Cao, A. and Gao, S.S. (2002) 'Temporal variation of seismic b -values beneath northeastern Japan island arc: TEMPORAL VARIATIONS IN B-VALUES', *Geophysical Research Letters*, 29(9), pp. 48-1-48–3. Available at: https://doi.org/10.1029/2001GL013775.

Hainzl, S. (2016) 'Rate-Dependent Incompleteness of Earthquake Catalogs', Seismological Research Letters, 87(2A), pp. 337–344. Available at: https://doi.org/10.1785/0220150211.

Hainzl, S. (2022) 'ETAS-Approach Accounting for Short-Term Incompleteness of Earthquake Catalogs', *Bulletin of the Seismological Society of America*, 112(1), pp. 494–507. Available at: https://doi.org/10.1785/0120210146.

Helmstetter, A., Kagan, Y.Y. and Jackson, D.D. (2006). Comparison of short-term and time-independent earthquake forecast models for southern California. *Bulletin of the Seismological Society of America*, 96(1), pp.90-106. Available at: https://doi.org/10.1785/0120050067

Lippiello, E. (2018) 'Spatiotemporal clustering of seismic occurrence and its implementation in forecasting models', In *Complexity of Seismic Time Series* (pp. 61-93). Elsevier. Available at: https://doi.org/10.1016/B978-0-12-813138-1.00003-1.

Nandan, S., Ouillon, G. and Sornette, D. (2019) 'Magnitude of Earthquakes Controls the Size Distribution of Their Triggered Events', *Journal of Geophysical Research: Solid Earth*, 124(3), pp. 2762–2780. Available at: https://doi.org/10.1029/2018JB017118.

Wiemer, S. (2000) 'Minimum Magnitude of Completeness in Earthquake Catalogs: Examples from Alaska, the Western United States, and Japan', *Bulletin of the Seismological Society of America*, 90(4), pp. 859–869. Available at: https://doi.org/10.1785/0119990114.

Woessner, J. (2005) 'Assessing the Quality of Earthquake Catalogues: Estimating the Magnitude of Completeness and Its Uncertainty', *Bulletin of the Seismological Society of America*, 95(2), pp. 684–698. Available at: https://doi.org/10.1785/0120040007.

Xiong, Q. et al. (2023) 'Seismic magnitude clustering is prevalent in field and laboratory catalogs', *Nature Communications*, 14(1), p. 2056. Available at: https://doi.org/10.1038/s41467-023-37782-5.